PMM Meeting
Oct 2018
Phoenix, AZ

Fingerprinting Orographic Precipitation Microphysics in Remote Sensing Measurements

Ana P. Barros, Malarvizhi Arulraj and Steven Chavez

Department of Civil and Environmental Engineering, Pratt School of Engineering, Duke University, NC

1. Physical Basis of Errors in GPM Ku-PR

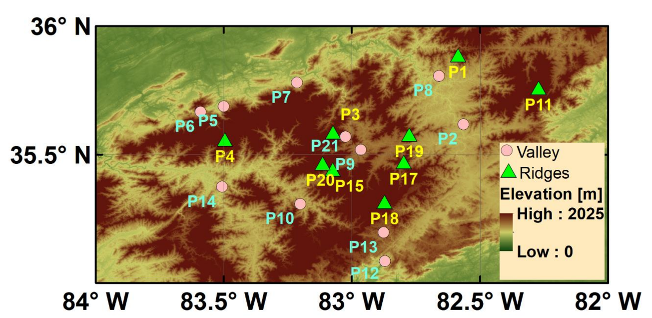

Figure 1: DEM of the Southern Appalachian Mountains (SAM) with locations of Ground Validation (GV) parsivel disdrometers. Ridges has DEM > 850 m.

Comparison of GPM Ku-PR estimates with long-term GV rain gauge suggests:
1. Robust temporal pattern of detection errors.
2. Underestimations when the GV rain-rate > 7 mm/h.

Physical Basis of Errors in QPE at Mountain Regions:

1. Contamination of near-surface reflectivities by ground-clutter (GC):

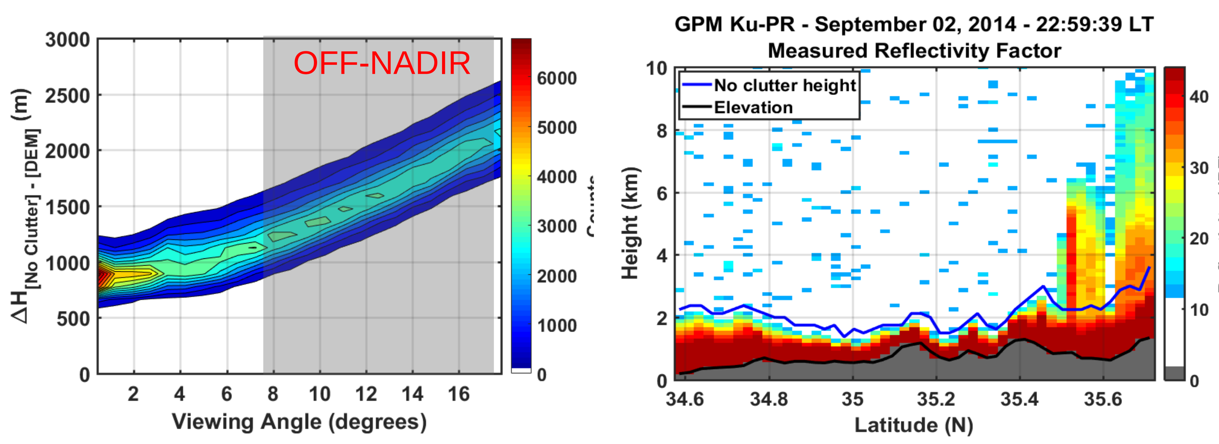

Figure 2: (a) Histogram of AGL height affected by ground-clutter (b) A swath of GPM Ku-PR measured reflectivity profiles showing the effect of ground-clutter.

For off-nadir cases , GC affects until 2.5 km AGL – leading to **underestimation of low-level enhanced rainfall.**

2. Error in DSD parameters – especially for Seeder-Feeder Interaction (SFI) cases

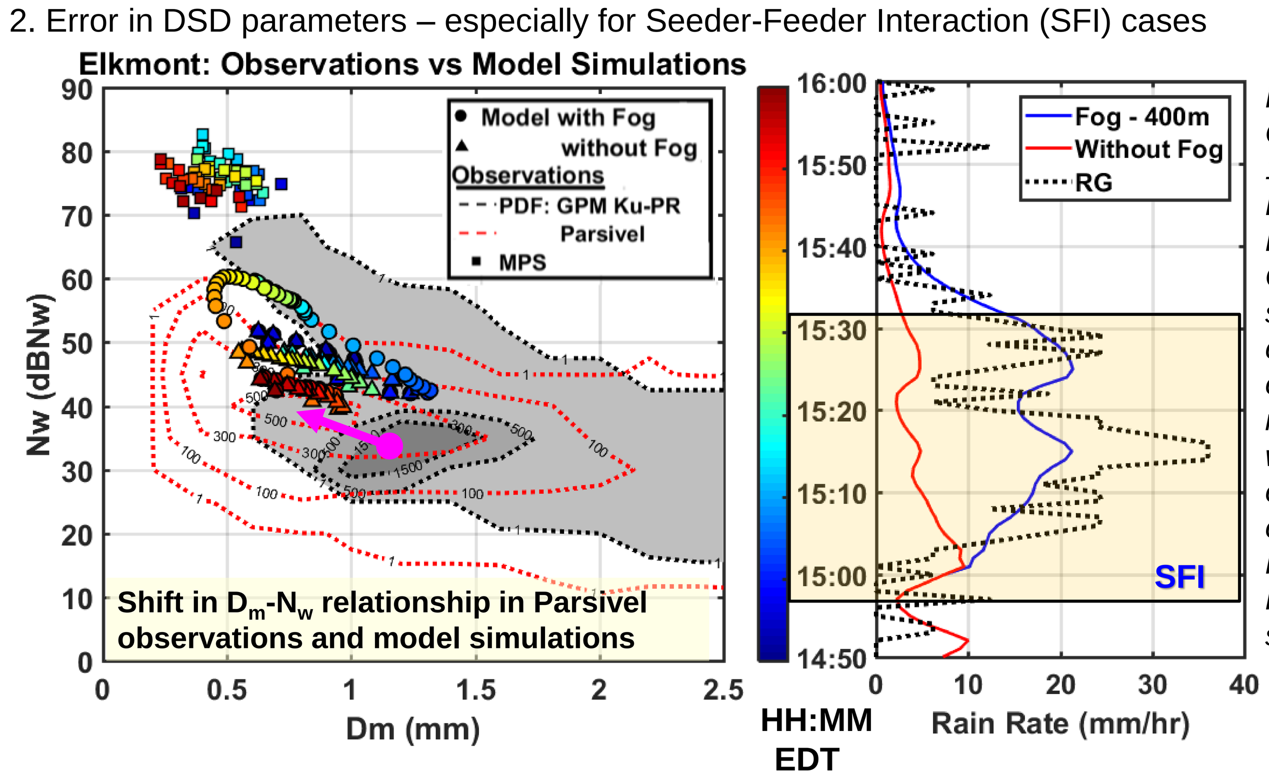

Figure 3: SFI observed on October 1, 2015 between 15:00 and 15:30 at Elkmont (P6 in Fig. 1). Duke Rain Microphysics Column Model was used to simulate this case using collocated MRR and MPS observations. (a) Dm-Nw relationship for with and without fog simulations over histogram of Parsivel observations and GPM Ku-PR. (b) Rain-rate from Rain-gauge and model simulations.

Warm Precipitation Case Study:

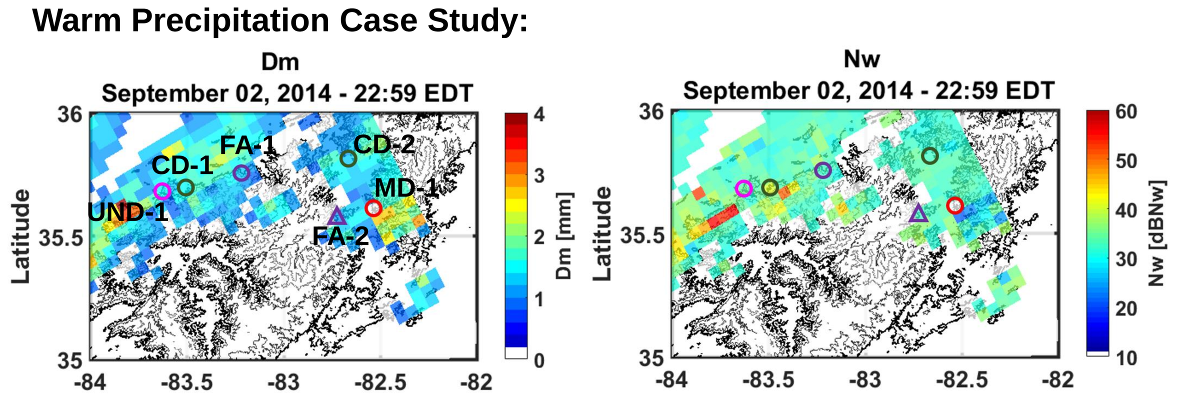

Figure 4: Spatial Distribution of D_m and N_w estimated by GPM Ku-PR in September 2, 2014. The collocated Parsivel locations and the corresponding error diagnostics are marked. UND, CD, FA and MD stands for underestimation, correct detection, false alarm and missed detection.

ID	Site	Rain-rate (mm/h)		D_m (mm)		N_w (dBNw)	
		Parsivel	Ku-PR	Parsivel	Ku-PR	Parsivel	Ku-PR
MD-1	P2 - valley	1.38	-	1.22	-	34.76	-
FA-1	P7 - valley	-	0.52	-	1.13	-	32.24
FA-2	P19 - ridge	-	0.66	-	1.18	-	32.43
UND-1	P6 – valley	10.41	2.51	1.48	1.45	39.54	34.01
CD-1	P5 – valley	11.24	10.20	1.87	1.41	35.23	40.78
CD-2	P8 - valley	1.65	1.73	1.31	1.36	34.39	33.59

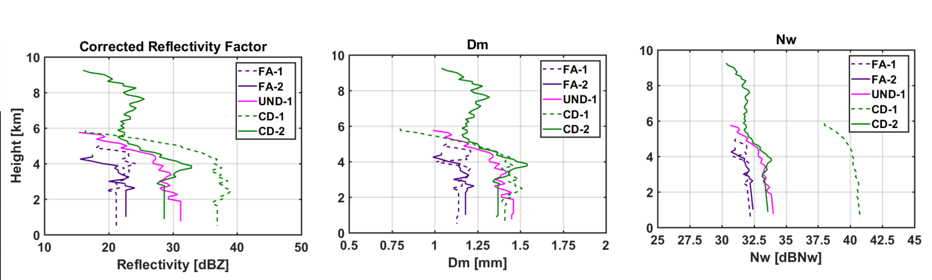

Table 1- Comparison of GPM Ku-PR estimates with collocated GV. Figure 5: Vertical profiles of corrected reflectivity factor, (b) D_m and (c) N_w from GPM Ku-PR.

GPM Ku-PR systematically underestimate Nw and rain-rate in the presence of low-level cloud and fog

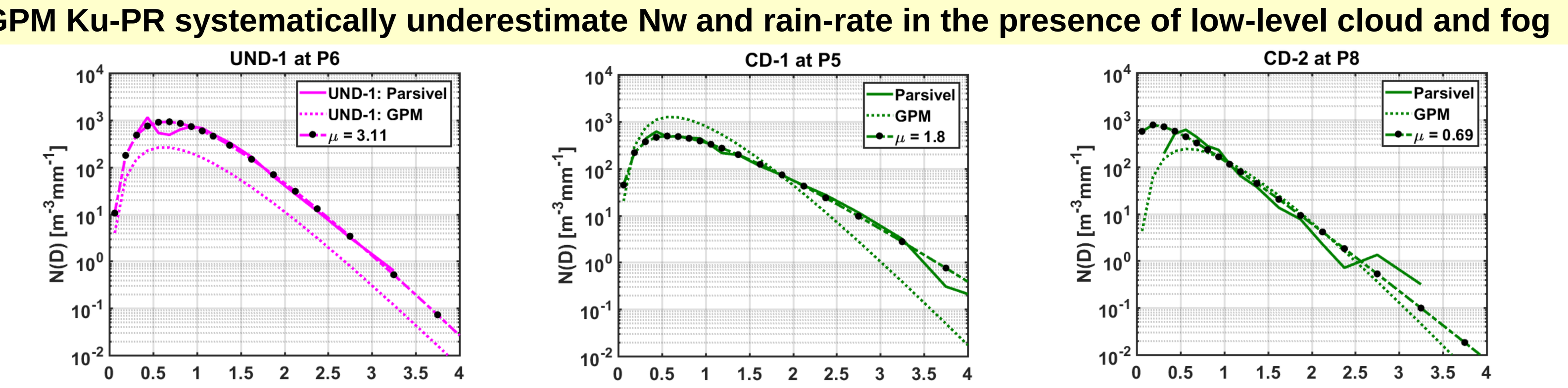

Figure 6: Comparison of DSD profiles from GPM Ku-PR with GV parsivel for the September 2, 2014 case. Dotted lines with markers are the best fit normalized gamma distribution function with Dm and Nw from parsivels.

The shape-parameter (μ) for Normalized Gamma distribution varies with the precipitation type.

2. Physical Model-based Correction Framework

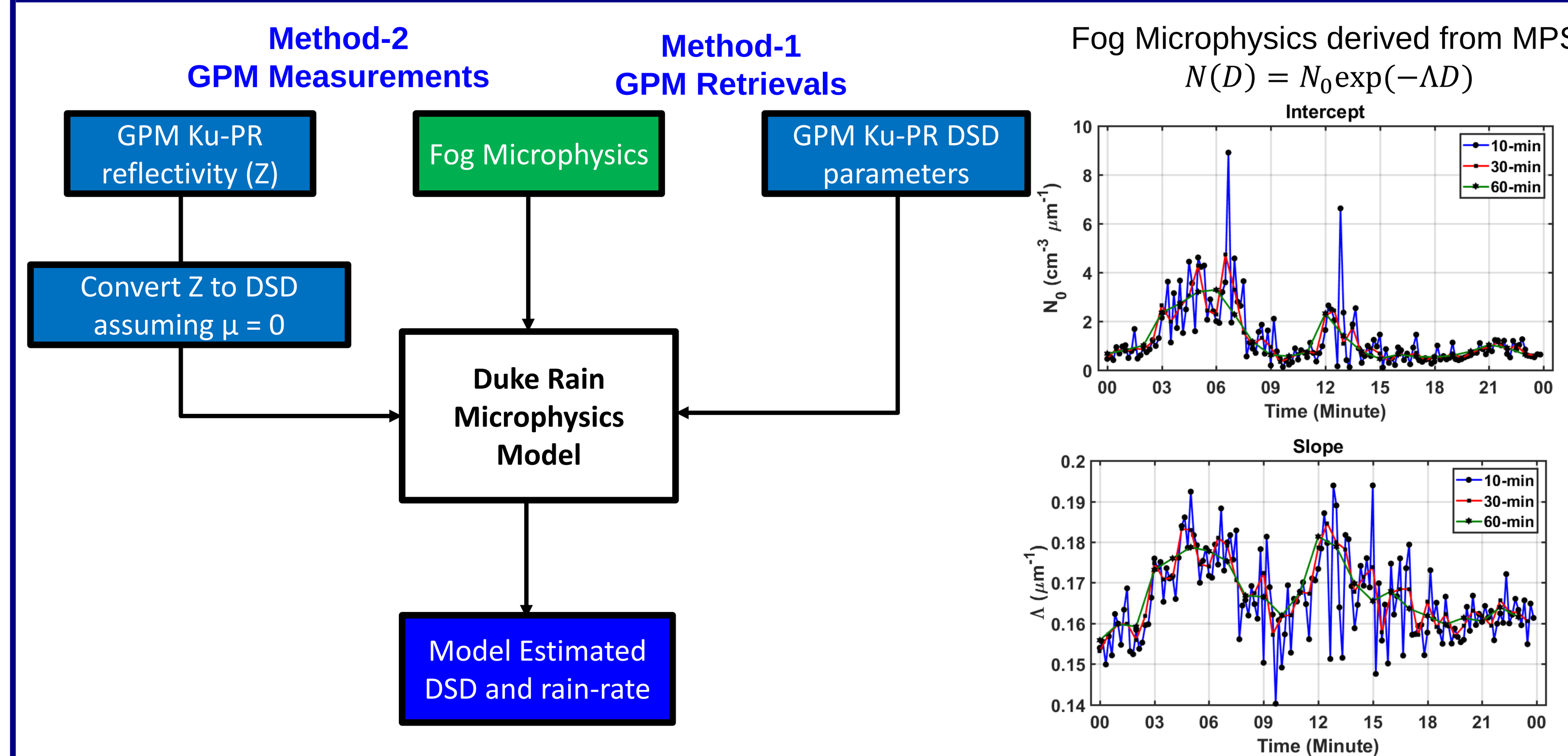

Figure 7 : (a)Schematic of the model-based correction framework. (b) Fog microphysics parameters from MPS observations at Elkmont (P6) when RG detects no rain and MPS detects fog used to represent fog in the model.

Model-based retrievals for underestimation cases:

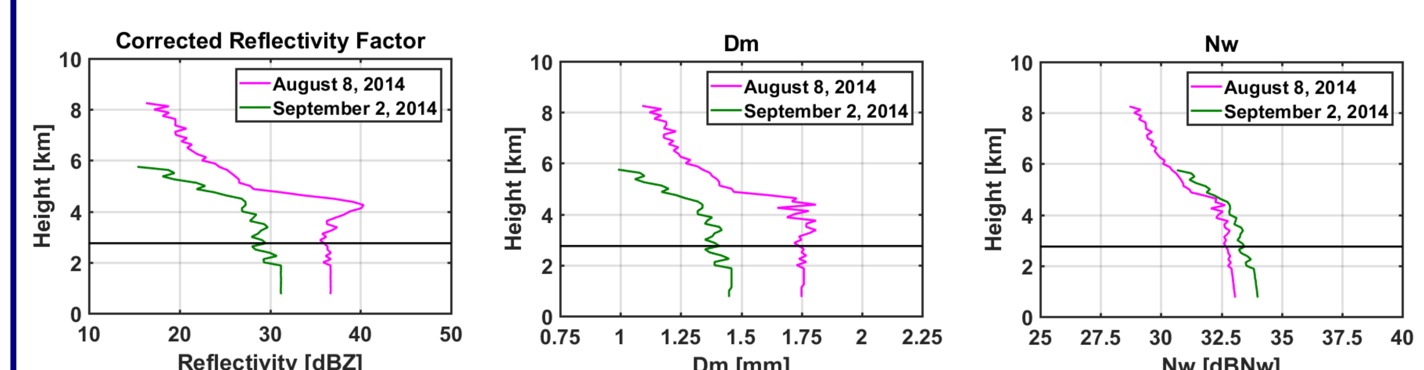

Figure 8: GPM Ku-PR estimated reflectivity profiles, Dm and Nw for two underestimation cases observed at the western foothills of the SAM. Black line denotes the location of the top boundary condition (2 km AGL).

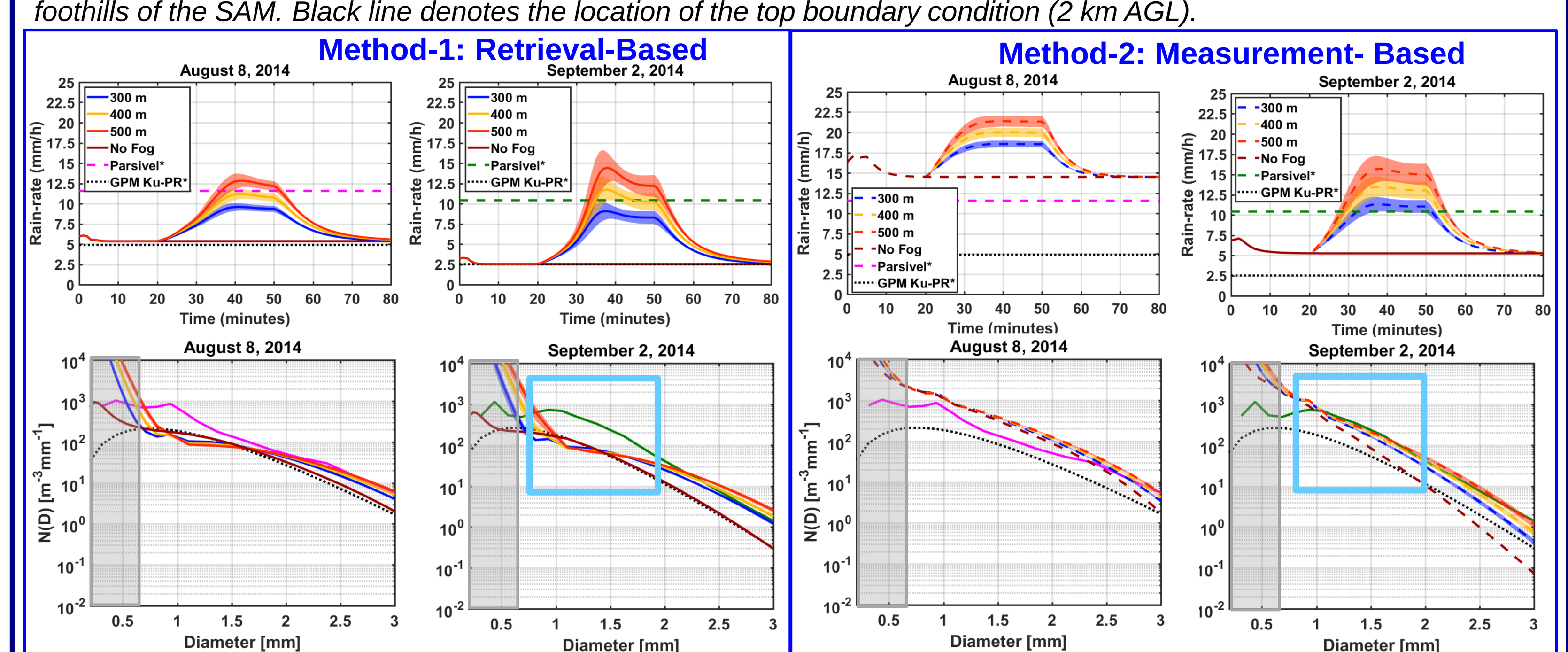

Figure 9: Simulated rain-rate and DSD spectra for Method-1 and Method-2 of the model simulations for the two underestimation cases. Low-level fog is forced between 20 and 50 minutes at three different depths.

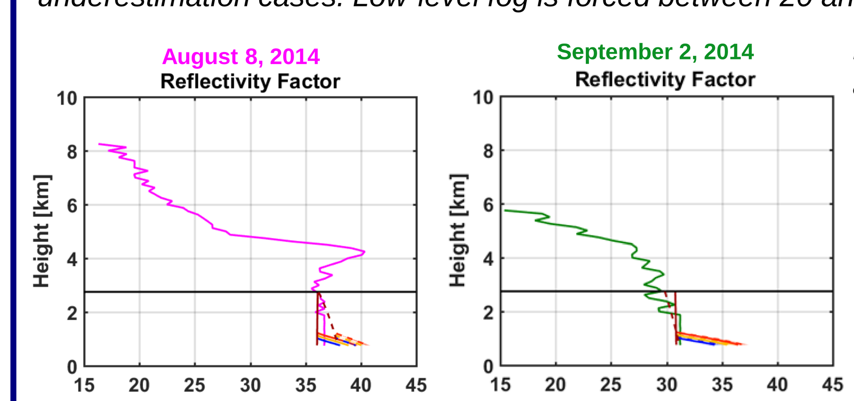

Figure 10: Reflectivity factor profiles from Model Simulations and GPM Ku-PR.

Findings:
1. Rain-rate from Method-1 without fog simulations match GPM Ku-PR estimates while the rain-rate from Method-2 without fog simulations are higher than the estimates.
2. DSDs between 0.75 and 1.5 mm are underestimated by Method-1 simulations. Method-2 DSDs are close to observations

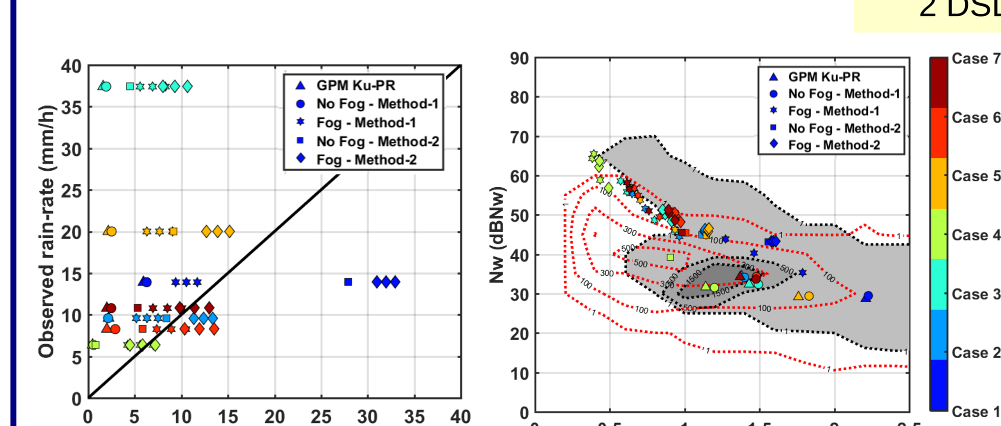

Figure 11: (a) Comparsion of rain-rate between the rain-gauge observations, GPM Ku-PR estimations and model simulations with and without low-level fog. (b) Dm-Nw relationship of GPM Ku-PR and Model simulations.

3. No-fog simulations from Method-2 are close to observations compared to Method-1 simulations.
4. Corrected Reflectivity Factors for Method-2 no-fog simulations also show low-level enhancement.

The model is also tested for seven underestimation warm precipitation cases in different regions of the SAM.

3. Orographic Precipitation – Central Andes

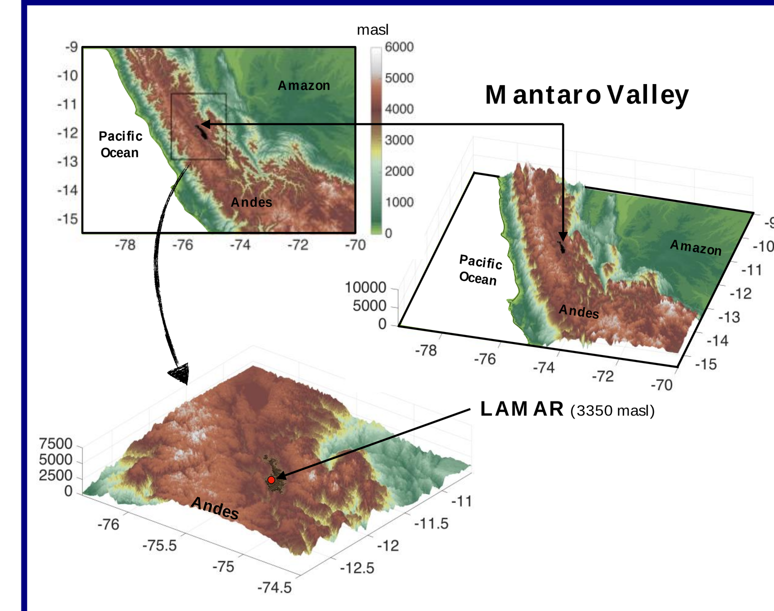

Figure 12: Digital elevation model of the Mantaro Valley in the Central Andes of Peru where the LAMAR Laboratory is located (red dot).

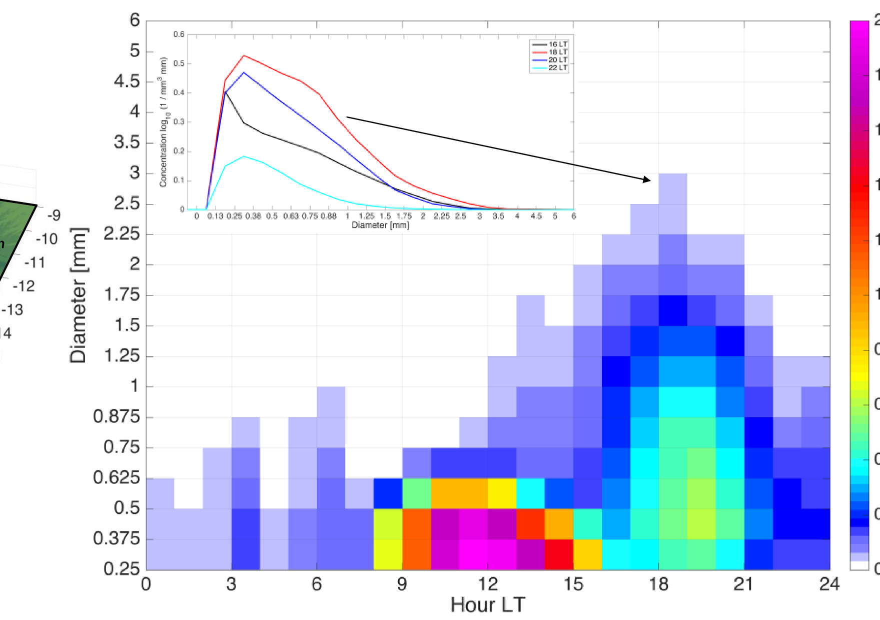

Figure 13: Drop size distribution from Parsivel2. The x-axis are the hours of the day, the y-axis is the diameter of the hydrometeors and in shading the concentration. In the superior left corner the drop size distribution for the period 16-22 LT as a plot where every hour is a different line.

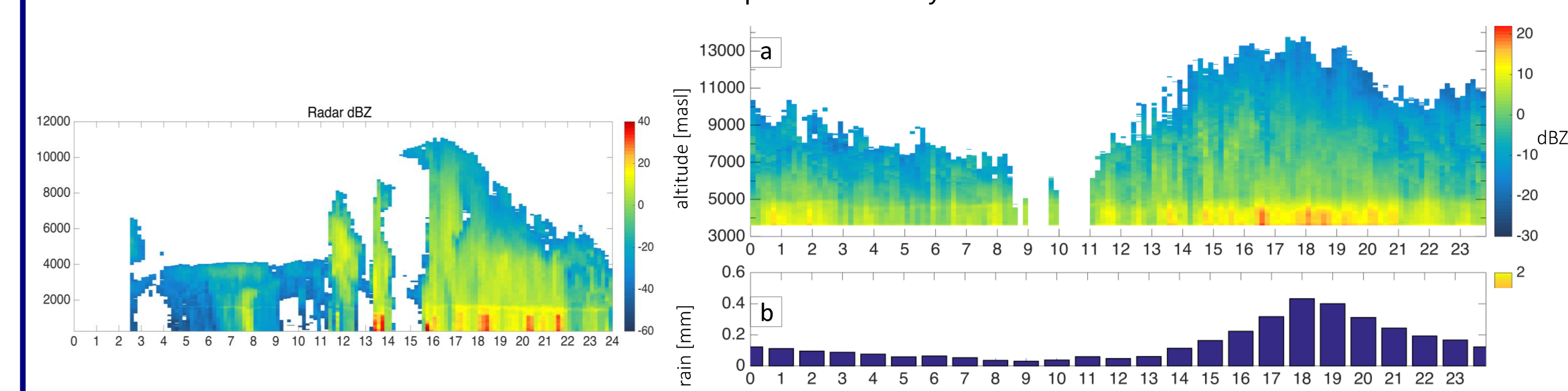

Figure 14 : Left panel – Ka- radar Reflectivity profiles at Mantaro Valley on February 3, 2016. Right Panel - a) 10-min averaged vertical profiles of reflectivity measured by a Ka Band radar Mira 35c when rains JFM 2016 and JF 2017. b) Mean diurnal cycle of precipitation measured by a rain-gauge.

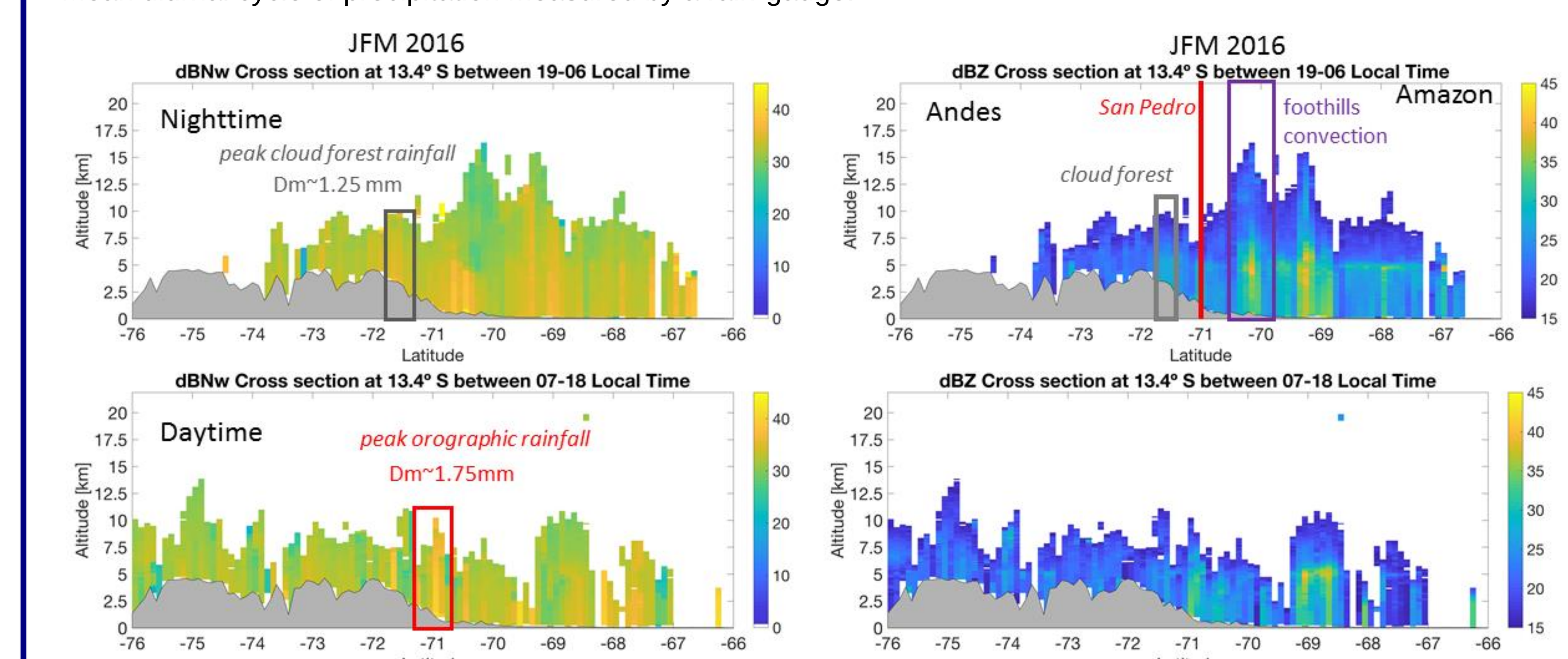

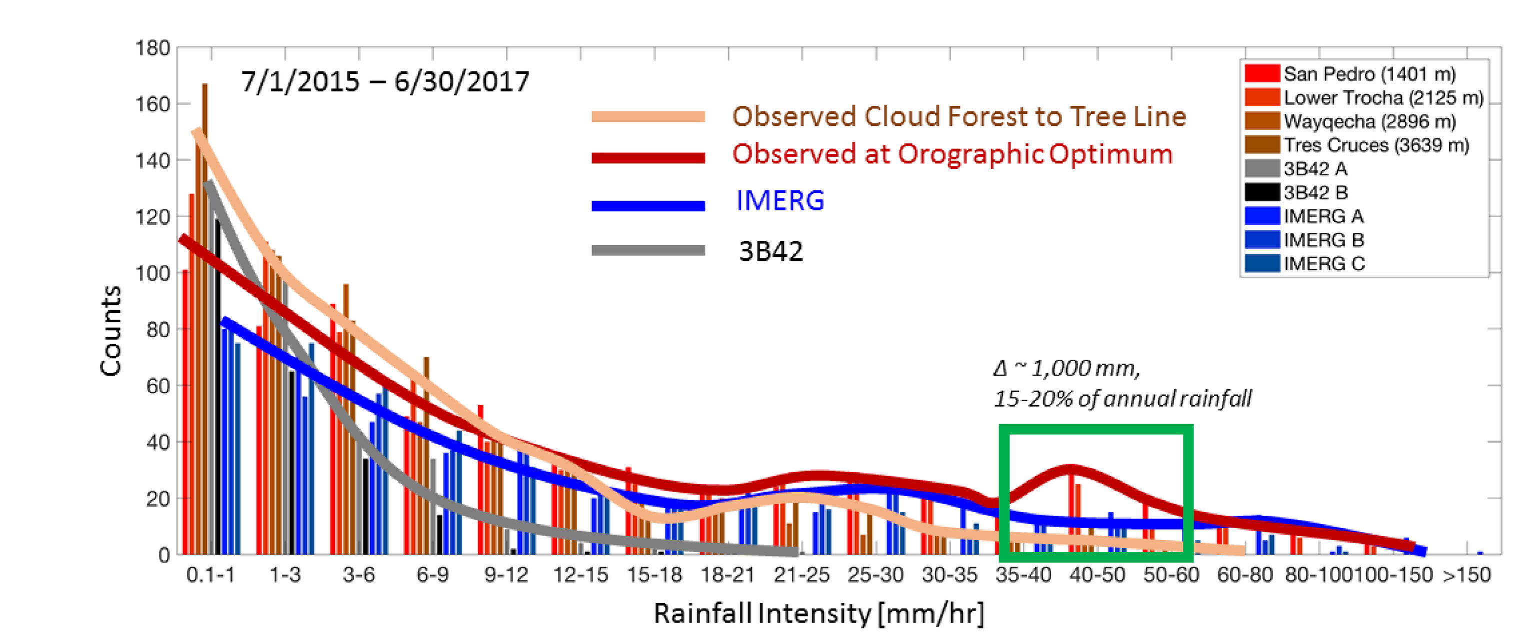

Figure 16 : Histogram of rainfall intensity observed along the rain gauge transect maintained by Duke University (DU) in the eastern Andes. Stations with incomplete records were removed. The letters A,B,C refer to different pixels of 3B42 and IMERG spanning the transect.

4. References and Acknowledgements

Chavez, S. P., and Takahashi K., 2017: Orographic rainfall hot spots in the Andes-Amazon transition according to the TRMM precipitation radar and in situ data, *J. Geophys. Res. Atmos.*, 122, 5870–5882, doi:10.1002/2016JD026282.

Duan,Y.,and Barros, A.P., 2017: Understanding how low-level clouds and fog modify the diurnal cycle of orographic precipitation using *in situ* and satellite observations, *Remote Sensing*, *9(9)*, 920; doi:10.3390/rs9090920.

Prat, O. P., and Barros, A. P., 2007: A Robust Numerical Solution of the Stochastic Collection–Breakup Equation for Warm Rain, *Journal of Applied Meteorology and Climatology*, 46, 1480-1497, 10.1175/jam2544.1.

–**Acknowledgments:** This research is supported by the NASA PMM program.